Scripta Materialia 132 (2017) 1–4

Contents lists available at ScienceDirect

Scripta Materialia

journal homepage: www.elsevier.com/locate/scriptamat

Regular article

Synthesis of ultra low temperature sinterable $Na_2Zn_5(MoO_4)_6$ ceramics and the effect of microstructure on microwave dielectric properties

J. Dhanya, A.V. Basiluddeen, R. Ratheesh *

Microwave Materials Group, Centre for Materials for Electronics Technology (C-MET), Department of Electronics and Information Technology, Government of India, Thrissur, Kerala 680581, India

ARTICLE INFO

Article history:
Received 26 December 2016
Received in revised form 12 January 2017
Accepted 12 January 2017
Available online xxxx

Keywords:
Energy dispersive X-ray spectroscopy
Electronic ceramics
Liquid-phase sintering
Grain growth
Ultra low temperature co-fired ceramic

ABSTRACT

Phase pure $Na_2Zn_5(MoO_4)_6$ ceramic is prepared by solid state ceramic route and the structural characterisations have been done using powder X-ray diffraction and laser Raman spectroscopy. $Na_2Zn_5(MoO_4)_6$ ceramics exhibited a maximum density of 3.73 g/cm^3 at 590 °C together with $\varepsilon_r = 8.1$, $Q_u \times f = 35{,}800$ GHz and $\tau_f = -95$ ppm/°C at microwave frequencies. Scanning electron micrographs of the sintered samples show exaggerated grain growth, which is correlated with the microwave dielectric properties. The chemical compatibility between $Na_2Zn_5(MoO_4)_6$ ceramic and metal electrode has been ascertained using energy dispersive X-ray spectroscopy.

Low-temperature co-fired ceramic technology has revolutionised the field of modern wireless communication systems [1]. Low temperature co-fired Ceramics (LTCC) substrates are much superior to conventional printed circuit boards and are widely used for the design and fabrication of high gain patch antennas, wide band filters, micro-electro-mechanical systems (MEMS), sensors and biomedical implants [2–6]. Ceramics that sinter below the melting point of silver (~961 °C), and which has got good chemical compatibility with silver electrode materials are termed as LTCC [3]. Sintering temperature of ceramics can be lowered by the addition of low melting glass phases or other sintering aids like CuO, B_2O_3, P_2O_5 and V_2O_5. However, glass free low-temperature sinterable ceramics are of much demand as the additives adversely affect the dielectric properties of the ceramics and increase the dielectric losses [7–9]. The critical materials requirement for co-firing applications are low dielectric constant, low loss tangent, low thermal coefficient of expansion and good chemical compatibility with metal electrodes. This class of ceramics substrates is prepared by multi-layer stacking technique wherein desired microwave circuits are screen printed within the ceramic layers using suitable cheap metal electrodes. High density integration of electronic components in a single low-loss LTCC module results in large scale miniaturisation of the microwave devices [1–6].

In order to further reduce the cost of multilayer devices, the new trend is to go for a new class of ceramics termed as ultra-low temperature co-firable ceramics (ULTCC) which sinters below 660 °C, the melting point of Al. The low processing temperature and cheaper electrode materials of ULTCC systems are expected to considerably improve the ease of device fabrication and reduce the cost of production. The low dielectric constant of such materials helps in improving the signal propagation delay and also enables them for high frequency microwave and millimeter wave applications since dielectric constant is inversely proportional to frequency of operation [10–12].

Among the materials envisaged, molybdate ceramics have been of particular interest for possible material system for ULTCC applications. $Li_8Bi_2Mo_7O_{28}$, Li_2MoO_4, $PbMoO_4$, $LiKSm_2(MoO_4)_4$, $CuMoO_4$, $Bi_2Mo_3O_{12}$, $Bi_2Mo_2O_9$, Ag_2MoO_4, $RE_2Mo_4O_{15}$ (RE = Nd, Sm), $K_2Mo_2O_7$, Na_2MoO_4 and $Na_2Mo_2O_7$ are some of the molybdate compositions reported for LTCC and ULTCC applications [13–21].

The title compound $Na_2Zn_5(MoO_4)_6$, a double molybdate, exists as triclinic phase in the Na_2MoO_4- $ZnMoO_4$ system (1:5 ratio). Klevtsova et al. reported the preparation of single crystals of $Na_2R_5(MoO_4)_6$(R = Mg, Zn, Co), and extensively studied the X-ray diffraction patterns [22]. In the present work, $Na_2Zn_5(MoO_4)_6$ ceramic is prepared by solid state ceramic route and its structural characterisation has been done using powder X-ray diffraction and laser Raman spectroscopic techniques. The microwave dielectric characterisation of the sintered ceramic compacts and chemical compatibility of the same with aluminium metal electrode have also been studied.

Conventional solid-state ceramic route was used to prepare phase pure $Na_2Zn_5(MoO_4)_6$ (hereafter referred as NZM) ceramics. The starting materials Na_2CO_3 (99%; Merck), ZnO (99%; Sigma Aldrich) and MoO_3 (99%; Himedia) were taken in stoichiometric proportions and mixed thoroughly in an agate mortar using distilled water as medium. The

* Corresponding author.
E-mail address: ratheeshr@yahoo.com (R. Ratheesh).
URL: http://www.cmet.gov.in (R. Ratheesh).

http://dx.doi.org/10.1016/j.scriptamat.2017.01.017
1359-6462/

slurry was dried at 100 °C in a hot air oven and ground well. The powder sample was then transferred into an alumina crucible and calcined at 500 °C for 1 h in a programmable SiC furnace. 5 wt. % PVA (Polyvinyl alcohol) binder was added to the finely ground calcined powder, dried and pressed into pellets in a 11 mm tungsten carbide die using a hydraulic hand press under a pressure of 200 MPa. The green pellets were sintered in the temperature range from 580 °C to 610 °C for 1 h to get required experimental density. The bulk density of the sintered samples was determined from dimensional methods.

Crystal structure and phase purity of the samples were studied by powder X-ray diffraction (XRD) measurement using a Bruker AXS model X-ray diffractometer with CuKα radiation. Carl Zeiss EVO 18 scanning electron microscope with energy dispersive X-ray spectroscopy (EDS) was used to study the surface morphology, as well as the chemical compatibility of the ceramic samples. Laser Raman spectrum of the composition was recorded using XploRA system equipped with an excitation wavelength of 532 nm, to understand the molecular structure. The shrinkage behaviour of the ceramic was studied using EXSTAR 6000 model Thermo Mechanical Analyzer (SII Nano technology INC., Japan). A Vector Network Analyser (Agilent make PNA E8362B, Bayan Lepas, Malaysia) was used to measure the microwave dielectric properties of the well sintered ceramics. The dielectric constant of the sample was measured by Hakki and Coleman post resonator technique [23] and the quality factor was measured by resonant cavity method [24]. The temperature coefficient of resonant frequency 'τ_f' of the ceramics was also measured in the temperature range 30–100 °C.

The powder X-ray diffraction pattern of NZM ceramic is shown in Fig. 1(a). The XRD pattern could be indexed only up to two theta value of 41° since the standard ICDD (International Centre for Diffraction Data) file no. 35-0312 is reported with hkl planes up to this. However, the XRD pattern of the sample under study is found to be exactly matching with the standard data. NZM ceramic crystallises in the triclinic crystal structure with space group $P\bar{1}$ [22].

The laser Raman spectrum of the NZM ceramic sintered at 590 °C for 1 h is given in Fig. 1(b). The crystal structure of NZM is reported to have Mo atoms in tetrahedral co-ordination [22]. The free-state MoO_4^{2-} tetrahedral structural units have four fundamental modes of vibration, namely, a non-degenerate symmetric stretching mode ν_1(A) at 894 cm^{-1}, a doubly degenerate symmetric bending mode ν_2(E) at 318 cm^{-1}, triply degenerate asymmetric stretching $\nu_3(F_2)$, and asymmetric bending $\nu_4(F_2)$ modes at 833 and 381 cm^{-1}, respectively [25–27]. The symmetric stretching vibrations (υ_1) of MoO_4^{2-} tetrahedra are observed as very strong peak at 937 cm^{-1} together with shoulder peak at 962 cm^{-1} and a weak mode at 917 cm^{-1}. Four bands are observed in the 888 to 789 cm^{-1} which corresponds to asymmetric stretching vibrations of MoO_4^{2-} ions. The symmetric (υ_2) and asymmetric (υ_4) bending vibrations of MoO_4^{2-} tetrahedra are appeared at 336 and 375 cm^{-1} respectively. The bands observed below 250 cm^{-1} can be attributed to lattice-mode vibrations and an unambiguous assignment of these modes is not possible [27].

The shrinkage behaviour of the NZM ceramic is shown in Fig. 1(c). It is clearly evident from the figure that the shrinkage rapidly increases beyond 400 °C, which clearly indicates that the ceramics under study can be well sintered within the ultra-low temperature range. In the present study, NZM ceramic is sintered in the temperature range from 580 °C to 610 °C to obtain maximum density. The density, dielectric constant and quality factor of NZM ceramic are plotted as a function of sintering temperature in Fig. 2(a). Both density and dielectric constant increase with increase in temperature, reach the maximum value at 590 °C and then start decreasing. The maximum sintered density obtained for NZM ceramics is 3.73 g/cm^3, which is about 92% of the theoretical density and the sample exhibits a dielectric constant (ε_r) of 8.1, quality factor ($Q_u \times f$) of 35,800 GHz, and temperature coefficient of resonant frequency (τ_f) of –95 ppm/ °C. The resonant frequency decreases with increase in temperature as shown in Fig. 2(b).

The SEM micrographs of NZM ceramics sintered at 590 °C and 600 °C for 1 h are shown in Fig. 2(c) and (d), with prominent grain sizes measured and labelled. NZM ceramic exhibits large polygonal grains with densely packed microstructure, which is comparatively rare in the case of liquid phase sintered ceramics. Unlike density and dielectric constant, the quality factor of NZM ceramic shows a maximum value for the sample

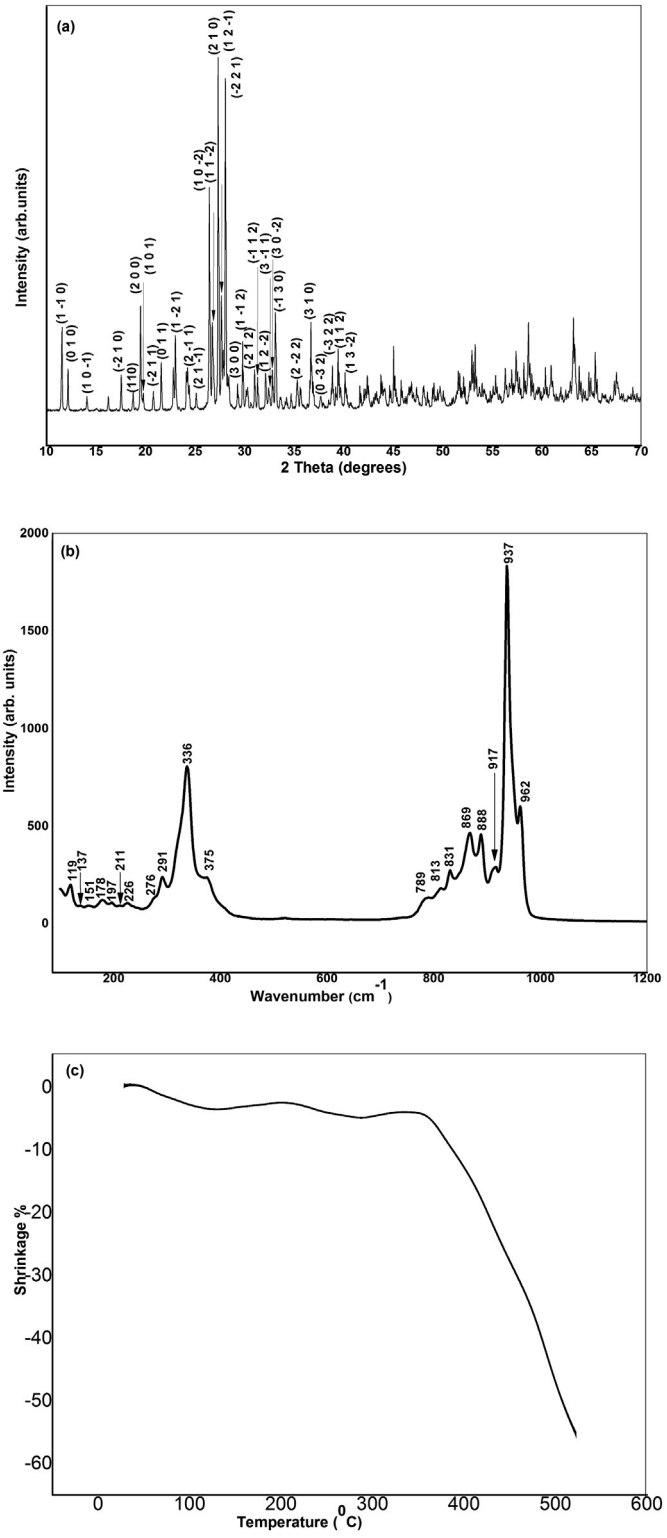

Fig. 1. (a) The X-ray diffraction pattern of $Na_2Zn_5(MoO_4)_6$ ceramics sintered at 590 °C for 1 h; (b) Raman spectrum of $Na_2Zn_5(MoO_4)_6$ ceramics sintered at 590 °C for 1 h; (c) Shrinkage behaviour of $Na_2Zn_5(MoO_4)_6$ ceramics.

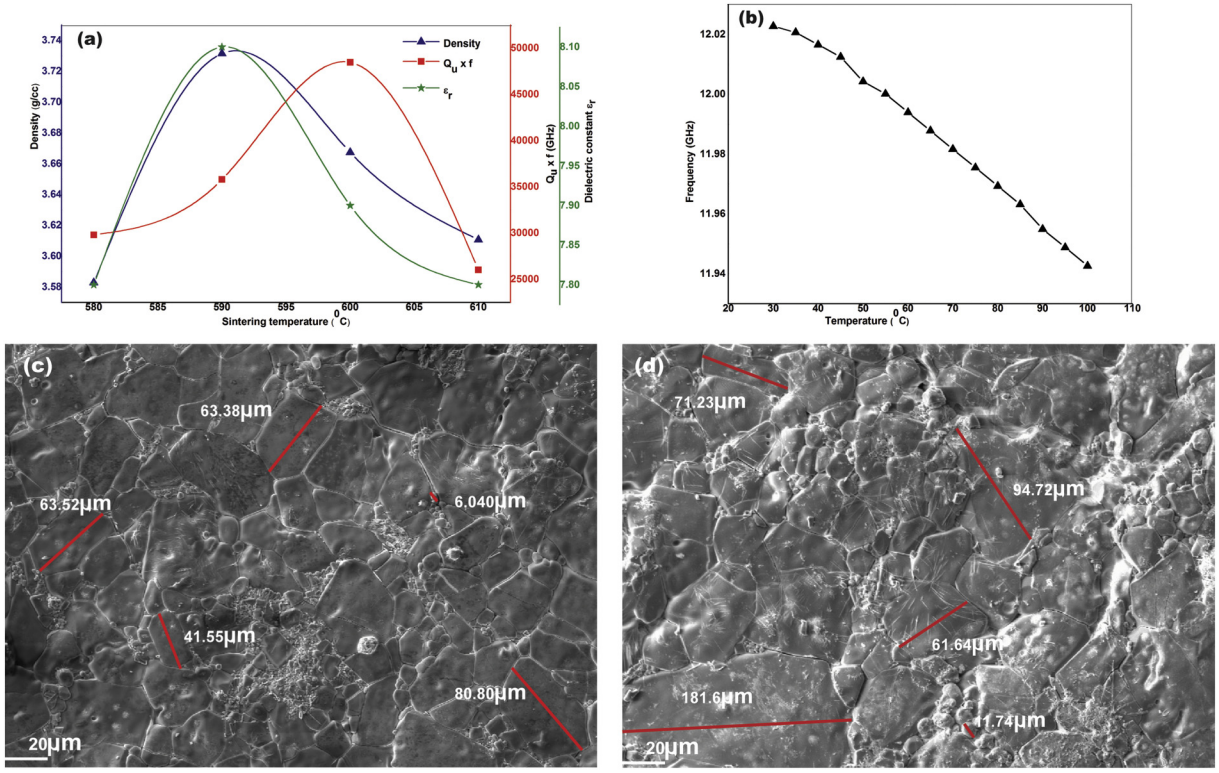

Fig. 2. (a) Variation in density, dielectric constant and quality factor of $Na_2Zn_5(MoO_4)_6$ ceramics with sintering temperature; (b) Variation in resonant frequency with temperature of $Na_2Zn_5(MoO_4)_6$ ceramics sintered at 590 °C for 1 h; (c) SEM micrograph of $Na_2Zn_5(MoO_4)_6$ ceramics sintered at 590 °C for 1 h with grain size labelled; (d) SEM micrograph of $Na_2Zn_5(MoO_4)_6$ ceramics sintered at 600 °C for 1 h with grain size labelled.

sintered at 600 °C, which can be correlated with the larger grain size compared with the sample sintered at 590 °C as shown in Fig. 2(c) and Fig. 2(d). Similar observations have been reported in the case of $Ba(Mg_{1/3}Ta_{2/3})O_3$(BMT) ceramics, wherein increase in grain size as a function of sintering time has led to decrease in grain boundary defects and dielectric losses with a remarkable increase in the quality factor [28–30].

The chemical compatibility of NZM ceramics with aluminium electrode is determined by co-firing the ceramic with 20 wt.% of aluminium powder at 590 °C for 1 h. The XRD pattern of the co-fired sample is shown in Fig. 3. The XRD pattern clearly exhibits the characteristic peaks of aluminium, as per ICDD file no. 89-2769 at 2θ values 38.5°, 44.7° and 65.1° marked with '*'. The pattern also contains all the peaks manifested in the XRD pattern of NZM ceramics given in Fig. 1(a), with no extra peaks as a result of Al addition, which clearly indicates the chemical compatibility of NZM with Al metal. The SEM images of the co-fired sample and the energy dispersive X-ray spectroscopy (EDS) point analysis have been done at aluminium region (spot 1) and ceramic region (spot 2) as shown in Fig. 4(a). The EDS spectra taken at spot 1 and spot 2 are shown in Fig. 4(c) and Fig. 4(d) respectively. The atomic weight percentage of each element is also given in the inset. The point analysis at the aluminium region clearly shows that there is very high degree of chemical compatibility between the aluminium electrode and the ceramic under study. The elemental colour mapping of the co-fired sample is given in Fig. 4(b). The aluminium region shown in green colour clearly depicts island formation surrounded by the ceramic grains and did not show any evidence of diffusion of aluminium into the ceramic region. It is also interesting to note that the aluminium addition hinders the growth of larger grains in the co-fired sample, resulting in uniform grain size of 1 to 5 μm, where as in the case of phase pure ceramic the grains have random size distribution varying up to 200 μm.

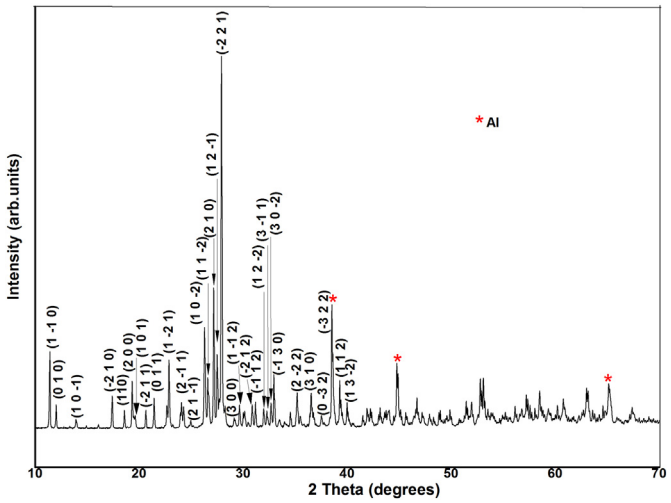

Fig. 3. XRD pattern of $Na_2Zn_5(MoO_4)_6$ ceramic cofired with 20 wt.% Al at 590 °C for 1 h.

In conclusion, phase pure $Na_2Zn_5(MoO_4)_6$ ceramic has been synthesised by solid state ceramic route. The prominent bands observed in the Raman spectrum are attributed to the normal modes of vibration of MoO_4^{2-} tetrahedra. The SEM micrograph shows dense microstructure with in homogeneous distribution of polygonal grains. The material under study exhibits rapid shrinkage behaviour beyond 400 °C. The ceramic compacts sintered at 590 °C show promising dielectric properties with $\varepsilon_r = 8.1$, $Q_u \times f = 35{,}800$ GHz and $\tau_f = -95$ ppm/°C at microwave frequencies. An increase in quality factor as a function of grain growth is noticed in the sample under study. The powder X-ray diffraction and EDS analysis show that the title compound has excellent chemical compatibility with aluminium metal electrode. Present study shows that $Na_2Zn_5(MoO_4)_6$ is a glass free, phase pure and cost effective microwave ceramic system ideal for ULTCC applications.

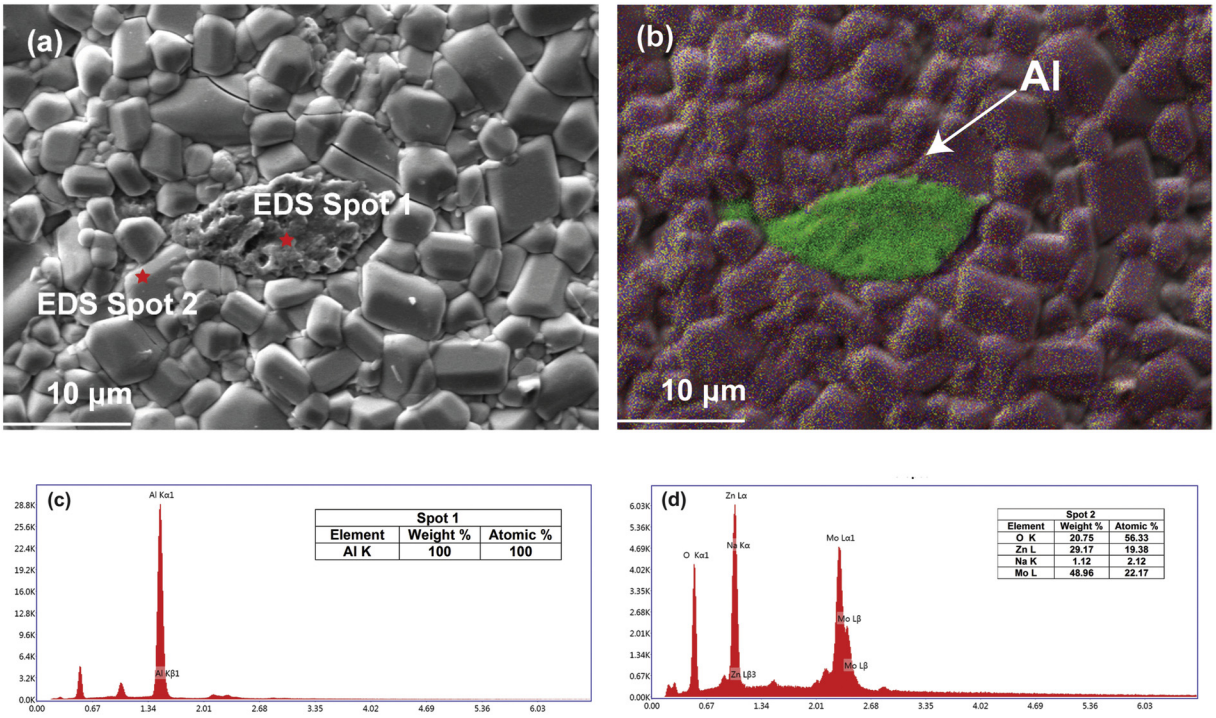

Fig. 4. (a) SEM image of $Na_2Zn_5(MoO_4)_6$ ceramic with 20 wt.% Al sintered at 590 °C for 1 h; (b) Elemental colour mapping of the $Na_2Zn_5(MoO_4)_6$ ceramic sintered with 20 wt.% Al; (c) EDS spectrum of spot 1 (d) EDS spectrum of spot 2.

Acknowledgement

The authors are thankful to Dr. N. Raghu, Director, C-MET, Thrissur for extending the facilities to the work. The authors are also thankful to the Board of Research in Nuclear Sciences, Mumbai for financial support under grant number 34/15/01/2014-BRNS/0906.

References

[1] I.M. Reaney, D. Iddles, J. Am. Ceram. Soc. 89 (2006) 2063–2072.
[2] J. Zhou, J. Adv. Ceram. 1 (2012) 89–99.
[3] M.T. Sebastian, H. Jantunen, Int. Mater. Rev. 53 (2008) 57–90.
[4] H. Yu, J. Liu, W. Zhang, S. Zhang, J. Mater. Sci. Mater. Electron. 26 (2015) 9414–9423.
[5] U. Ullah, M.F. Ain, N.M. Mahyuddin, M. Othman, Z.A. Ahmad, M.Z. Abdullah, A. Marzuki, IEEE Antennas Propag. Mag. 57 (2015) 241–260.
[6] Y.-S. Lin, C.-C. Liu, K.-M. Li, C.H. Chen, IEEE Trans. Microwave Theory Tech. 52 (2004) 2718–2724.
[7] C.-L. Huang, M.H. Weng, H.L. Chen, J. Mater. Chem. Phys. 71 (2001) 17–22.
[8] A.Y. Borisevich, P.K. Davies, J. Am. Ceram. Soc. 87 (2004) 1047–1052.
[9] D. Zhou, H. Wang, L.-X. Pang, X. Yao, Mater. Chem. Phys. 119 (2010) 149–152.
[10] M.T. Sebastian, H. Wang, H. Jantunen, Curr. Opin. Solid State Mater. Sci. 20 (2016) 151–170.
[11] E.K. Suresh, A.N. Unnimaya, R. Ratheesh, J. Am. Ceram. Soc. 97 (2014) 1530–1533.
[12] A.N. Unnimaya, E.K. Suresh, R. Ratheesh, Eur. J. Inorg. Chem. 2 (2015) 305–310.
[13] D. Zhou, C.A. Randall, H. Wang, L.-X. Pang, X. Yao, J. Am. Ceram. Soc. 93 (2010) 1096–1100.
[14] H.H. Xi, D. Zhou, B. He, H.D. Xie, J. Am. Ceram. Soc. 95 (2014) 1375–1378.
[15] X.-L. Zhai, X. Zheng, H.-H. Xi, W.-B. Li, J. Han, D. Zhou, J. Am. Ceram. Soc. 98 (2015) 2716–2719.
[16] N. Joseph, J. Varghese, T. Siponkoski, M. Teirikangas, M.T. Sebastian, H. Jantunen, ACS Sustain. Chem. Eng. 4 (2016) 5632–5639.
[17] D. Zhou, H. Wang, L.-X. Pang, C.A. Randall, X. Yao, J. Am. Ceram. Soc. 92 (2009) 2242–2246.
[18] D. Zhou, W.-B. Li, L.-X. Pang, J. Guo, Z.-M. Qi, T. Shao, Z.-X. Yue, X. Yao, J. Am. Ceram. Soc. 97 (2014) 3597–3601.
[19] A. Surjith, E.K. Suresh, S. Freddy, R. Ratheesh, J. Mater. Sci. Mater. Electron. 24 (2013) 1818–1822.
[20] G.-Q. Zhang, J. Guo, L. He, D. Zhou, H. Wang, J. Koruza, M. Kosec, J. Am. Ceram. Soc. 97 (2014) 241–245.
[21] G.-Q. Zhang, H. Wang, J. Guo, L. He, D.-D. Wei, Q.-B. Yuan, J. Am. Ceram. Soc. 98 (2015) 528–533.
[22] R.F. Klevtsova, V.G. Kim, P.V. Klevtsov, Sov. Phys. Crystallogr. 25 (1980) 657–660.
[23] B.W. Hakki, P.D. Coleman, IRE Trans. Microwave Theory Tech. 8 (1960) 402–410.
[24] J. Krupka, K. Derzakowski, B. Riddle, J.B. Jarvis, Meas. Sci. Technol. 9 (1998) 1751–1756.
[25] F.D. Hardcastle, I.E. Wachs, J. Phys. Chem. 95 (1991) 10763–10772.
[26] F.D. Hardcastle, I.E. Wachs, J. Raman Spectrosc. 21 (1990) 683–691.
[27] N.K. James, R. Ratheesh, J. Am. Ceram. Soc. 93 (2010) 931–933.
[28] N. Ichinose, T. Shimada, J. Eur. Ceram. Soc. 26 (2006) 1755–1759.
[29] D.J. Barber, K.M. Moulding, J. Zhou, M.Q. Li, J. Mater. Sci. 32 (1997) 1531–1544.
[30] C.-L. Huang, K.-H. Chiang, S.-C. Chuang, Mater. Res. Bull. 39 (2004) 629–636.